Published in final edited form as:
Biomaterials. 2011 April ; 32(11): 2834–2850. doi:10.1016/j.biomaterials.2011.01.012.

The mechanical coupling of adult marrow stromal stem cells during cardiac regeneration assessed in a 2-D co-culture model

Mani T. Valarmathi[*], **John W. Fuseler**, **Richard L. Goodwin**, **Jeffrey M. Davis**, and **Jay D. Potts**

Department of Cell Biology and Anatomy, School of Medicine, University of South Carolina, Columbia, SC 29209, USA

Abstract

Postnatal cardiomyocytes undergo terminal differentiation and a restricted number of human cardiomyocytes retain the ability to divide and regenerate in response to ischemic injury. However, whether these neo-cardiomyocytes are derived from endogenous population of resident cardiac stem cells or from the exogenous double assurance population of resident bone marrow-derived stem cells that populate the damaged myocardium is unresolved and under intense investigation. The vital challenge is to ameliorate and/or regenerate the damaged myocardium. This can be achieved by stimulating proliferation of native quiescent cardiomyocytes and/or cardiac stem cell, or by recruiting exogenous autologous or allogeneic cells such as fetal or embryonic cardiomyocyte progenitors or bone marrow-derived stromal stem cells. The prerequisites are that these neo-cardiomyocytes must have the ability to integrate well within the native myocardium and must exhibit functional synchronization. Adult bone marrow stromal cells (BMSCs) have been shown to differentiate into cardiomyocyte-like cells both in vitro and in vivo. As a result, BMSCs may potentially play an essential role in cardiac repair and regeneration, but this concept requires further validation. In this report, we have provided compelling evidence that functioning cardiac tissue can be generated by the interaction of multipotent BMSCs with embryonic cardiac myocytes (ECMs) in two-dimensional (2-D) co-cultures. The differentiating BMSCs were induced to undergo cardiomyogenic differentiation pathway and were able to express unequivocal electromechanical coupling and functional synchronization with ECMs. Our 2-D co-culture system provides a useful in vitro model to elucidate various molecular mechanisms underpinning the integration and orderly maturation and differentiation of BMSCs into neo-cardiomyocytes during myocardial repair and regeneration.

Keywords

Bone marrow stromal cells; Mesenchymal stem cells; Embryonic cardiac myocytes; Dedifferentiation; Myocardial regeneration; Cardiac tissue engineering

[*]Corresponding author. Building 1 Room B-31, 6439 Garners Ferry Road, Department of Cell Biology and Anatomy, School of Medicine, University of South Carolina, Columbia, SC 29209, USA. Tel.: +1 803 216 3821; fax: +1 803 733 3153. valarmathi64@hotmail.com, valarmathi.thiruvanamalai@uscmed.sc.edu (M.T. Valarmathi).

Disclosures

All authors have no conflicts of interest.

1. Introduction

Mammalian heart has been considered as a post-mitotic organ composed of highly specialized and terminally differentiated cardiac myocytes. These mammalian cardiac myocytes have traditionally been considered as post-mitotic cells with an extremely low or practically no capacity to divide and regenerate [1]. However, lower vertebrates such as fish and amphibians retain a substantial capacity for myocardial regeneration. In both adult frogs and newts the differentiated cardiac myocytes have the ability to undergo mitotic division after damage to the heart [2–4]. This regeneratory process involves a partial cellular dedifferentiation (i.e. the loss of most contractile filaments) of the myocytes before the initiation of mitotic cycle [5]. Recently, it has been shown that mammalian cardiac muscle has limited proliferative potential and restricted regeneration within the damaged myocardium [6,7]. Hence, it may be beneficial to explore the limited natural capacity of mammalian cardiac muscle regeneration in light of the spontaneous cardiac muscle regeneration observed in these lower vertebrate animals [8].

The difficulty in regenerating damaged myocardial tissue has led researchers to explore the application of embryonic- and/or adult derived stem cells as possible sources for regenerating myocardium [9–12]. Using stem cells, it has been possible to stimulate mammalian cardiac muscle regeneration and researchers have investigated the potential of adult bone marrow stromal cells (BMSCs) for cardiac tissue repair and/or regeneration [13–15]. BMSCs are multipotent, capable of differentiating into the main cardiac cell lineages such as myocytes, endothelial and vascular smooth muscle cells in vitro and contribute to myocardial regeneration in vivo when transplanted to the failing heart following myocardial infarction or non-infarction in mouse, rat, pig or sheep models [16–19]. Additionally, the ability of BMSCs to restore functionality may be enhanced by the simultaneous transplantation of other stem and progenitor cells [20]. Finally, the significant advantage of using these BMSCs is their low immunogenicity. And BMSCs have been reported to be immunomodulatory and immunotolerogenic both in vitro as well as in vivo [21]. Taken together, these facts suggest that BMSCs may represent the cell of greatest potential for adult autologous and/or allogeneic stem cell based cardiac regeneration.

Restoring damaged heart muscle tissue, through repair or regeneration, therefore represents a fundamental mechanistic strategy to treat congestive heart failure. However, current emerging clinical studies using stem cells, including BMSCs to repair damaged cardiac tissue have produced varying results [22,23]. On the one hand, irrespective of the modes of administration, the marrow stem cells contributed to cardiac repair in vivo and prevented ventricular remodeling and alleviated cardiac symptoms; on the contrary, there occurred reduction in cardiac blood flow (myocardial ischemia) or pronounced congestive heart failure [13,24]. These reports clearly indicate that there exist gaps in the knowledge base pertaining to adult stem cell based cardiac regeneration, and much remains to be resolved for the successful translation of stem cell based cellular cardiomyoplasty from bench to bedside. Thus, elucidation of various molecular mechanisms underpinning the integration and orderly maturation and differentiation of BMSCs into neo-cardiomyocytes during myocardial repair and regeneration necessitates the development of appropriate in vitro two-dimensional (2-D) and three-dimensional (3-D) models of cardiomyogenesis [15].

In this study, we tested the hypothesis that whether functioning cardiac tissue can be generated by the interaction of putative multipotent BMSCs and embryonic cardiac myocytes (ECMs) in a 2- D co-culture condition. In this co-culture condition, BMSCs underwent maturation and differentiation characteristic of myogenic lineage, which was evidenced by the expression of the cardiac phenotype and by electromechanical coupling with the developing ECMs.

2. Materials and methods

2.1. BMSCs isolation, expansion and maintenance

Procedures were performed in accordance with the guidelines for animal experimentation by the Institutional Animal Care and Use Committee (IACUC), School of Medicine, University of South Carolina. Rat BMSCs were isolated from the bone marrow of adult 300 g Sprague Dawley®™ SD®™ rats (Harlan Sprague Dawley, Inc.) as described previously [25]. Briefly, after deep anesthesia, the femoral and tibial bones were removed aseptically and cleaned extensively to remove associated soft connective tissues. The marrow cavities of these bones were flushed with Dulbecco's Modified Eagle Medium (DMEM; Invitrogen) and combined. The obtained marrow plugs were triturated, and passed through needles of decreasing gauge (from 18 gauge to 22 gauge) to break up clumps and cellular aggregates. The resulting single-cell suspensions were centrifuged at 200 g for 5 min. Nucleated cells were counted using a Neubauer chamber. Cells were plated at a density of 5×10^6–2×10^7 cells per T75 cm^2 flasks in basal media composed of DMEM supplemented with 10% fetal bovine serum (FBS, lot-selected; Atlanta Biologicals, Inc.), gentamicin (50 μg/ml) and amphotericin B (250 ng/ml) and incubated in a humidified atmosphere of 5% CO_2 at 37 °C for 7 days. The medium was replaced, and changed three times per week until the cultures became ~70% confluent (between 12 and 14 days). Cells were trypsinized using 0.05% trypsin–0.1% EDTA and re-plated at a density of 1×10^6 cells per T75 cm^2 flasks. After three passages, attached marrow stromal cells were devoid of any non-adhering population of cells.

2.2. Immunophenotyping of BMSCs by flow cytometry and confocal microscopy

Qualitative evaluation for various cell surface markers was performed on cells grown in the Lab-tek™ chamber slide system™ (Nunc) using a Zeiss LSM 510 Meta confocal scanning laser microscope (Carl Zeiss, Inc.) and quantitative analysis of the same set of surface markers was performed by single-color flow cytometry using a Coulter® EPICS® XL™ Flow Cytometer (Beckman Coulter, Inc.) as described previously [26]. Briefly, the passage 3 maintained BMSCs were trypsinized, pelleted at 200 g for 5 min and washed twice with Mosconas's solution, pH 7.4. Cells were resuspended in staining buffer (1.5% bovine serum albumin in PBS, pH 7.4) (BSA, Sigma–Aldrich) and incubated for 30 min at 4 °C with appropriate dilutions of FITC-conjugated mouse anti-rat CD11b, CD31, CD44, CD45, CD90 and OX43 monoclonal antibodies for direct immunostaining (Table 1). Similarly, the cells were incubated with FITC-unconjugated mouse anti-rat CD34, CD73 and CD106 monoclonal antibodies followed by incubation with appropriate dilutions of FITC-conjugated antimouse secondary antibodies for indirect immunostaining (Table 1). FITC-labeled mouse anti-rat-IgGs antibodies served as the isotype controls. The stained cells were washed twice with Moscona's solution and the data acquired immediately or alternately the

cells were fixed in ice-cold 0.5% paraformaldehyde (Sigma–Aldrich) and stored in the dark at 4 °C until acquired in flow cytometry. Finally, the obtained data were analyzed using Expo32 ADC software (Beckman Coulter, Inc.).

2.3. Purification and enrichment of CD90$^+$ BMSCs by magnetic-activated cell sorting (MACS)

The adherent populations of BMSCs were further purified by indirect magnetic cell labeling method using an autoMACS™ Pro Separator (Miltenyi Biotech) as described previously [26]. The cells were subjected to CD90 positive selection by incubating the cells with FITC-labeled anti-CD90 antibodies (BD Pharmingen), followed by incubation with anti-FITC magnetic microbeads (Miltenyi Biotech), and passed through the magnetic columns as per the manufacturer's instructions. The resultant enriched CD90$^+$/CD34$^-$/CD45$^-$ fractions were expanded by subcultivation and subjected to flow cytometric analysis.

2.4. Labeling of BMSCs with green or red fluorescent protein (GFP or RFP) for lineage tracing

2.4.1. Lentiviral vectors and lentivirus production—Lentiviral construct generation and lentivirus preparation were performed as described previously [15]. In brief, lentiviral expression plasmid pWPI-GFP or pWPI-RFP, along with packaging plasmid pCMVΔR8.91 and envelope plasmid pMD.D(VSV-G) were co-transferred with a mass ratio of 3:2:1 into a 30–40% confluent 293T cells in serum-free medium using ProFection® Mammalian transfection system (Promega) following the manufacturer's instructions. The transfected cells were incubated in a humidified atmosphere of 5% CO_2 at 37 °C for 16 h. After 16 h, the serum-free medium was replaced with fresh DMEM medium supplemented with 10% FBS to collect viral particles for the next 24 h. The collected viral supernatants were filtered through 0.22 μm, pooled and subjected to ultracentrifugation at 26,000 rpm using an SW28 rotor for 2 h. The supernatant was removed and the deposited viral particles were resuspended in 100 μl of PBS, pH 7.4 and stored at −70 °C until further use. The viral titer was determined by standard HeLa titre procedure using GFP or RFP as a marker.

2.4.2. Lentiviral transduction—For lentiviral transduction, BMSCs (0.2×10^6 cells/well) and the desired number of viral particles (MOI = 5) were resuspended in 1 ml of serum-free medium (serumfree DMEM) and were seeded onto six-well culture plates precoated with retronectin (20 μg/ml/well) and incubated overnight in a humidified atmosphere of 5% CO_2 at 37 °C. After overnight transduction, the serum-free medium was replaced with complete medium (DMEM with 10% FBS) and cells were further incubated for 48–72 h before the transduced GFP or RFP gene expression was analyzed. The GFP or RFP marked BMSCs were expanded further by subculturing. GFP or RFP expression was observed using confocal microscopy and the transduction efficiency was estimated by flow cytometry (>95%).

2.5. Embryonic cardiac myocytes (ECMs) isolation

Isolation of embryonic ventricular primary cells was performed as described in detail previously [15,27] with modifications. Briefly, under deep euthanasia, E15 timed pregnant Sprague Dawley®™ SD®™ rats (Harlan Sprague Dawley, Inc.) were subjected to cervical

dislocation and the embryos were removed from the adherent placental membranes. The hearts were dissected out from these E15 embryos and pooled in ice-cold Moscona's solution. Atria were removed from the ventricles under a dissecting microscope (Olympus SZ60) and discarded. Isolated ventricles were rinsed with ice-cold Krebs–Ringer bicarbonate-I (KRB-I) with 1 mg/ml BSA fractionV, 2 mg/ml glucose, 100 U/ml penicillin, and 75 U/ml streptomycin, pH 7.4. The ventricles were minced thoroughly and incubated with a KRB-II-collagenase type II (Worthington) solution (120 U/ml) in a 37 °C shaking water bath. Tissues were dissociated by repeated triturations (at 8 min intervals). The process was repeated until all tissues were completely dissociated. Then, the cells were pelleted at 800 g for 8 min, the supernatant was discarded, and the obtained pellet was resuspended in 5 ml of KRB-II solution (20 mg/ml BSA fractionV, 2 mg/ml glucose, 100 U/ml penicillin, and 75 U/ml streptomycin, pH 7.4) and passed through a 20 μm nylon mesh. The cells were once again pelleted and resuspended in complete myocyte medium composed of DMEM (4.5 g/L glucose, L-glutamine and sodium pyruvate; Cellgro by Mediatech, Inc.) supplemented with 8% horse serum (HS, lot-selected, Gibco®), 5% newborn calf serum (NCS, Atlanta Biologicals, Inc.), penicillin (100 U/ml), streptomycin (100 μg/ml) and amphotericin B (1 μg/ml). Further, to remove the co-existing cardiac fibroblasts the above cell suspensions were plated in 100mmcell culture dishes and incubated in a humidified atmosphere of 5% CO_2 at 37 °C for 30 min. Following incubation, the non-adherent myocytes were slightly tapped and aspirated off immediately from the panning dishes and, the procedure was repeated two more times. After panning, the cells were once again pelleted and resuspended in myocyte medium.

2.6. ECMs only culture

Isolated ventricular primary cells were quantified using a hemocytometer and plated at a density of 2×10^5 cells/35 mm glass bottom culture dishes precoated with monolayer of collagen (MatTek Corporation). Cells were seeded into the wells of glass bottom culture dishes, incubated in a humidified atmosphere of 5% CO_2 at 37 °C for 48 h, and observed under microscope for spontaneous beating and rhythmicity. These ECMs (ECMs only) were cultured in complete myocyte medium (DMEM with 8% HS and 5% NCS) for further 6, 12, or 18 days.

2.7. BMSCs and ECMs co-culture

The expanded and purified population of $CD90^+$ BMSCs (GFP unlabeled or GFP labeled) were seeded onto the surface of the previously generated ECM culture wells (after 48 h) at a density of 0.4×10^5 cells/35 mm glass bottom culture dishes and cultured in complete myocyte medium for 6, 12, or 18 days. The cultures (ECMs/BMSCs-GFP unlabeled or ECMs/BMSCs-GFP labeled or ECMs only) were terminated at these regular intervals and the collected samples were subjected to RT-qPCR, immunofluorescent staining, calcium transit imaging, contractility, morphometric and ultrastructural analyses.

2.8. Contractility assay and calcium flux assay

2.8.1. Calcium imaging using fluorescent probes by confocal microscopy—

Preparation of Fluo-4 calcium indicator: The Fluo-4 calcium indicator (50 μg, Molecular Probes, Invitrogen) was reconstituted initially with 15 μl of anhydrous dimethylsulfoxide

(DMSO, Sigma–Aldrich), followed by the addition of 3 μl of Pluronic F–127 (Molecular Probes, Invitrogen) in 20% DMSO. This constituted 18 μl of concentrated (~2.5 mM) stock solution of Fluo-4. Once prepared, this solution should preferably be used within 48 h. The working solution of Fluo-4 was prepared by diluting the stock solution 1:2000 in Moscona's buffer.

2.8.2. Loading of cells with Fluo-4 or Calcium Orange Calcium indicators— Single-cell Ca^{2+} imaging technique was employed for the recording of changes in the intracellular Ca^{2+} flux of differentiating cells. The cultures (ECMs only or BMSCs-RFP only or ECMs/BMSCs-RFP labeled) maintained on 35 mm glass bottom culture dishes (MatTek Corporation) were terminated at regular intervals (day 6 or day 12) and the cells were washed twice with Moscona's solution, pH 7.4 (to remove the serum and phenol red, the pH indicator from the tissue culture medium as it will interfere with the calcium indicator, Fluo-4). The cells were incubated with 2000 μl of Fluo-4 working solution and incubated at 37 °C for 30 min. Following incubation, the Fluo-4 solution was gently removed and the samples were washed twice with Mosconas's buffer. Then, the cells were replenished with 2 ml of myocyte medium (phenol red free) and incubated for further 30 min. In particular, the calcium indicator Calcium Orange was used in lieu of Fluo-4, when GFP labeled BMSCs were employed for co-culture experiments. The reagent preparation and the labeling method was essentially the same as that employed for Fluo-4.

2.8.3. Live cell imaging using confocal laser scanning microscope—The calcium indicator (Fluo-4 or Calcium Orange) loaded cell culture dishes were maintained in an environmental chamber (humidified atmosphere of 5% CO_2 and 37 °C) mounted on the stage of a Zeiss inverted fluorescence microscope (Axiovert 200M) equipped with a CARV spinning disk confocal attachment. All types of cells were imaged with a Zeiss 20×, NA = 0.75 FLUAR objective, and images were captured by a CCD camera (Hamamatsu ORCA-ER) controlled by Kinetic Imaging Image Acquisition Software (AQM Advance-6) software. All images were recorded at constant exposures using the following filter sets: FITC (490/515) for Fluo-4 calcium expression and TRITC (555/570) for RFP expression; or, FITC (490/515) for GFP expression and TRITC (555/570) for Calcium Orange expression. Images were captured at 500 ms intervals of 2 to 5 min duration. Minimal photo bleaching was encountered while capturing the images. Background fluorescence was minimal or non-detectable in these sample images. Changes in intracellular calcium flux were determined by measuring the changes in mean intensity of the Fluo-4 or Calcium Orange fluorescence within a selected region of interest (ROI) within the cell cytoplasm by using the AQM Advance-6 software.

2.8.4. Morphometric analysis of cell shape changes and morphological transformation—Changes in cell shape and morphology of both BMSCs and ECMs over time were analyzed by using the integrated morphometry subroutine of MetaMorph 6.1. (Universal Imaging Corp, Downingtown, PA). Briefly, the 24 bit color images were color separated into red (BMSC-RFP) and green (Fluo-4 calcium in BMSCs and ECMs) channels and these individual images were converted into 8 bit monochrome images. Complete BMSCs or ECMs in the 8 bit monochrome image field were isolated and thresholded as

regions of interest (ROI). In each frame, alterations in cell shape were determined by measurement of the changes of the elliptical form factor (EFF). The EFF was defined as the ratio of the breadth (caliper width of the cell perpendicular to the longest chord, B) to the length (longest chord through the major axis of the cell, L), thus, EFF = L/B. Changes in intracellular calcium were determined by measuring the changes in the intensity of the Fluo-4 or Calcium Orange fluorescence and, changes in cellular movement was determined by measuring the displacement of the margin of the cell or selected particle within the cell passed a fixed point or defined region using the AQM Advance-6 software.

2.9. Real-time polymerase chain reaction (mRNA quantification by RT-qPCR)

Total cellular RNA extraction from three independent cultures (ECMs/BMSCs- GFP unlabeled or ECMs only) maintained inmyocyte medium were performed using TRIzol® Plus RNA purification kit (Invitrogen) according to manufacturer's instructions. The quality and quantity of the obtained RNA was analyzed on the Agilent 2100 Bioanalyzer using the Agilent RNA 6000 nano kit (Agilent Technologies, Inc.) according to manufacturer's instructions. The reverse transcriptase (RT) reaction was performed using 250 ng of total RNA in a final reaction volume of 20 μl using an iScript™ cDNA synthesis kit (Bio-rad Laboratories) according to manufacturer's recommendations. Gene-specific primers for cardiac myosin heavy chain alpha (myosin, heavy chain6, cardiac muscle, alpha - Myh6/α-MHC), cardiac myosin heavy chain beta (myosin, heavy chain 7, cardiac muscle, beta - Myh7/β-MHC), cardiac α-actin (actin, alpha, cardiac muscle 1 – Actc1), cardiac troponin I (troponin I type 3, cardiac - Tnni3, cTnI), GATA binding protein 4 (Gata4), atrial natriuretic peptide (natriuretic peptide precursor A – Nppa/ANP), brain natriuretic peptide (natriuretic peptide precursor B – Nppb/BNP) and connexin 43 (gap junction protein, alpha 1 – Gja1/C× 43) and; the endogenous normalizer reference gene, acidic ribosomal phosphoprotein P0 (Arbp) were designed using web based software Primer3 [28], synthesized commercially (Integrated DNA Technologies, Inc.), and evaluated for an annealing temperature of 58 °C as shown in Table 2.

Real-time PCR conditions were optimized as described previously [25]. All RTqPCRs were performed with SYBR Green I chemistry in a MyiQ™ single-color realtime PCR detection system (Bio-rad Laboratories). For qPCRs, iQ5 SYBR Green I supermix, 3 pmol/μl of each forward and reverse primers, and 5 μl cDNA template were used in a final reaction volume of 50 μl. PCR cycling parameters included an initial denaturation of 8 min and 45 s at 95 °C followed by 45 cycles of 30 s at 95 °C, 30 s at 58 °C, and 30 s at 72 °C. Data collection was enabled at 72 °C in each cycle. C_T (threshold cycle) values were calculated using the MyiQ optical system software, version 2.0. The calibrator control included BMSCs day 0 sample and the target gene expression was normalized by a non-regulated reference gene expression, Arpb. The mathematical model previously described in detail [29], was used to determine the expression ratio of genes.

2.10. Immunofluorescence staining and confocal microscopy

Cultures (ECMs/BMSCs-GFP labeled or ECMs only) samples were collected at day 6, 12, or 18 and processed according to previously described protocols [30]. After incubation, the cultured cells were rinsed twice in Mosconos's solution, pH 7.4 and fixed in 2%

paraformaldehyde at 4 °C for 12–16 h. Each of the samples was then permeabilized in PBS, pH 7.4 containing 0.1% Triton X-100 and 100 mM glycine for 30–40 min at room temperature and blocked in 1.5% BSA, 100 mM glycine in PBS for 1 h at room temperature. The primary antibodies used are shown in Table 1. Primary antibodies were used at 1:200 dilutions in blocking buffer for 12–16 h at 4 °C. Secondary antibodies (Alexa fluor® 488 and 546 obtained from Molecular Probes, Invitrogen) were used at 1:200 dilutions in blocking buffer for 2 h at room temperature in the dark. Nuclei were stained with DAPI (4, 6-diamidino-2-phenylindole, 100 ng/ml; Sigma–Aldrich). Images of the stained cells were visualized using a confocal microscope (Zeiss LSM 510 Meta CSLM). Negative controls for staining included only secondary antibodies.

2.11. Transmission electron microscopic (TEM) analysis

To visualize the ultrastructural characteristics of the co-differentiating cells, day 18 samples were processed for transmission electron microscopy (TEM) as described previously with modifications [15]. In brief, the wells of Permanox Lab-tek™ chamber slide system™ (Nunc) that were seeded with cells (BMSCs only or ECMs only or BMSCs/ECMs) and cultured inmyocyte medium were rinsed twice in PBS, pH 7.4. The cells were fixed in 2.5% glutaraldehyde (Sigma–Aldrich) in PBS overnight at 4 °C, and rinsed in PBS. The samples were then post fixed in 1% OsO_4 and 1.5% potassium ferricyanide in PBS for 1 h at room temperature, rinsed in water, and dehydrated through a graded ethanol series up to 100%. Then, the samples were impregnated with increasing concentrations of PolyBed 812 up to pure resin, using acetonitrile as an intermediate solvent, embedded and cured at 60 °C for two days. The embedded samples were cut on an ultramicrotome (Leica Ultracut R) and 100 nm sections were collected on Cu grids. The sections were then stained with 2% uranyl acetate for 40 min at 37 °C, and Hanaichi lead stain for 6 min at room temperature and examined using a JEOL200CX TEM (Tokyo, Japan) operated at 120 kV. Images were captured using Axiovision, Software Engine Version 5.42.479 by AMT (Advanced Microscopy Techniques, Danvers, MA).

2.12. Statistical analysis

Morphometric data were represented as mean ± standard deviation of the mean (mean ± SD). The RT-qPCR data were represented as mean ± standard error of the mean (mean ± SEM) and, the differences in expression (cardiomyogenic markers) between control (day 0) and treated samples (day 6, 12, or 18) were assessed ingroup means for statistical significance by applying '*Pair Wise Fixed Reallocation Randomization Test*' using Relative Expression Software Tool (REST®) [29]. In all cases, values of $p < 0.05$ were considered statistically significant.

3. Results

3.1. Phenotypic characterization of undifferentiated BMSCs

Immunophenotyping of undifferentiated BMSCs for various cell surface markers by flow cytometry revealed that the fluorescent intensity and distribution of the cells stained for CD11b, CD31, CD44 and CD45 were not significantly different from the intensity and distribution of cells stained with isotype controls (Fig. 1A–C,E,F). In addition, these cells

were negative for the rat endothelial cell surface marker OX43 (Fig. 1J), an antigen expressed on all vascular endothelial cells of rat, indicating that these cultures were devoid of any hematopoietic stem and/or progenitor cells as well as differentiated bone-marrow-derived endothelial cells. In contrast, BMSCs exhibited a high expression of CD73 (93.77%) and CD90 (99.85%) surface antigens (Fig. 1G–H), which are consistent characteristics of undifferentiated BMSCs. Phenotypic characterization using the same set of markers on BMSCs by confocal microscopy also revealed that the cells were negative for CD11b, CD31, CD34, CD44, CD45, CD106, OX43 and, strongly positive for CD73 and CD90 (data not shown). The expression profiles of these surface molecules were consistent with previous reports and the minimal criteria for defining multipotent mesenchymal stromal cells, set forth by the international society for cellular therapy (ISCT) position statement [26,31,32].

3.2. Cellular morphology, morphometry and contractility

The cell cultures that contained exclusively BMSCs and were grown in myocyte medium assumed a general morphological phenotype of an oblate spheroid with an EFF of 2.409 ± 0.248. Whereas, BMSCs that were co-cultured with ECMs expressed phenotypic changes in morphology. Within 24 h of seeding, BMSCs were able to tether to the juxtaposed ECMs and were able to demonstrate synchronous cellular movement at the same frequency as the spontaneously and rhythmically beating ECMs. Following seven days of co-culture revealed that BMSCs have become mechanically attached to the ECMs and deformed by cyclic stretching at the same frequency essentially dictated and exerted by the contractions of adjacent ECMs (Fig. 2A–F). Morphological changes in BMSCs included cyclic changes in length (Fig. 3A) and changes in breadth (Fig. 3B). The change in breadth appeared to be variable and only partially associated with the cyclic changes in length. BMSCs, which were mechanically attached to the spontaneously and rhythmically contracting ECMs also became elongated assuming the morphology of prolate spheroid with an EFF of 3.552 ± 0.167, which was significantly greater ($p < 0.001$) than the EFF of 2.409 ± 0.248 characteristic of BMSCs (quiescent) that were either in non co-culture condition or not in physical contact with ECMs in co-culture condition. The EFF of BMSC that was mechanically associated with ECMs was not invariant but undergone cyclic changes dictated by the contraction frequency of the adjacent ECMs (Fig. 3C). The EFF of BMSC that was in non co-culture conditions and/or not associated with ECMs in co-culture conditions exhibited non-cyclic changes associated with normal cellular movements and migration (Fig. 3D).

3.3. Cellular calcium flux

BMSCs co-cultured in the presence of spontaneously beating and rhythmically contracting ECMs and that were mechanically coupled to ECMs revealed intracellular calcium fluxes characterized by cyclic oscillations (Fig. 4A,B,E,F). The calcium flux seen in the case of BMSC, which was mechanically connected to a contracting ECM, when imaged over a time intervals of 5 min or greater exhibited calcium peaks at frequency similar or equal to that of the ECM (Fig. 4C,D,E,F). The amplitude of the intracellular calcium oscillations seen in BMSC that was actively and mechanically associated with an ECM ($\Delta Ca^{2+} = 13.88 \pm 7.57$) was significantly greater ($p < 0.001$) than that seen in a BMSC, which was quiescent and not attached to an ECM ($\Delta Ca^{2+} = 3.84 \pm 2.32$), but is significantly less ($p < 0.001$) than the

calcium flux associated with myofibrillar contractions seen in the case of spontaneously and synchronously beating ECM (ΔCa^{2+} = 127.52 ± 40.55).

Examination of the intracellular calcium fluxes induced in BMSCs by mechanical interaction with a single ECM over shorter time intervals (2–3 s) provided additional more detailed resolution of this response (Fig. 5A–F). The non co-cultured BMSCs also demonstrated non-rhythmic contractions with minimal flux of intracellular calcium as seen in normal cellular migrations and movement (negative control, Fig. 5A). Calcium induced Fluo-4 fluorescence was essentially random with an average mean intensity (ΔCa^{2+}) of 3.84 ± 0.06 (Fig. 5A) and significantly different from the calcium flux associated with myofibrillar contractions in ECM (Fig. 5B). An individual BMSC that was mechanically coupled with a single ECM exhibited intracellular calcium flux with frequency (Fig. 5C), which was almost identical to the frequency of calcium flux recorded in the ECM (Fig. 5D). When two individual BMSCs were in mechanical coupling with the same individual ECM but not in direct contact with each other, the frequency and amplitude of their intracellular calcium flux was almost identical (Fig. 5E). The pattern and frequency of the intracellular calcium flux in these two separate BMSCs was same as that seen in the case of ECM (Fig. 5F).

3.4. mRNA analysis of cardiomyogenic markers

To determine the differential gene expression profiles between BMSCs/ECMs co-culture and ECMs only culture, real-time quantitative RT-PCR (RT-qPCR) analyses of cardiogenic differentiation markers were carried out at the defined time points (6, 12, and 18 days) on BMCSs/ECMs co-cultured in myocyte medium. Additionally, RT-qPCR on ECMs cultured in the same medium condition was performed at the same time points.

ECMs cultured in myocyte medium constitutively expressed transcripts coding for key cardiogenic lineage specific markers (Fig. 6A,C). The structural and contractile filamental associated genes, α-MHC, β-MHC, β-Actc1 and cTnI showed remarkable upregulation up to 18 days with concurrent progressive gradual downregulation of these transcripts over the observed time period (Fig. 6A). In addition, in ECMs cultures, the transcript levels of Gata4, Nppa and Nppb demonstrated a sustained upregulation up to 18 days with a noticeable kinetics of gradual downregulation of these transcripts over the successive experiential time points (Fig. 6C). In contrast, in BMSC/ECM co-cultures the expression pattern of key cardiogenic marker transcripts showed moderate differences in their expression profile, especially the structural and contractile filamental genes.

ECMs/BMSCs co-cultured in myocyte medium expressed the cardiogenic differentiation related marker transcripts consistently. The structural and contractile filamental associated genes, α-MHC, β-MHC, α-Actc1 and cTnI showed sustained high levels of expression until day 18 with simultaneous gradual downregulation of these marker transcripts during each successive time points (Fig. 6B). Besides, in BMSCs/ECMs co-cultures, the transcript levels of Gata4, Nppa and Nppb showed notable upregulation over 12 days and there exist a continual gradual downregulation of these transcripts over the observed consecutive time points (Fig. 6D). On the contrary, the connexon gene, Gja1 transcripts showed gradual upregulation up to 18 days.

3.5. Expression of cardiomyogenic markers in ECMs and GFPBMSCs/ECMs cultures

To validate the findings of mRNA expression and to determine whether these upregulated cardiac specific messages were in fact getting translated into proteins, immunofluorescent staining of various key cardiomyogenic phenotypic markers was explored on these ECMs and GFP-BMSCs/ECMs cultures.

3.5.1. Characterization of ECMs in ECMs only culture—Immunostaining of these differentiating cells using antibodies directed against cardiac specific transcription factors, structural and contractile filaments, hormones and junctional complex proteins were carried out. Immunostaining and confocal laser scanning microscopic analysis established that these ECMs only culture were composed of cells that were positive for a variety of cardiomyocyte specific markers, cardiac α/β-myosin heavy chain (α/β-MHC), sarcomeric myosin heavy chain (sMHC), cardiac troponin I (cTnI), desmin, connexin 45 (C×45), connexin 43 (C×43), GATA-binding protein 4 (Gata4) and brain natriuretic peptide (BNP). Representative staining patterns obtained for these cardiac-related proteins for ECMs only cultures are shown in Fig. 7(A–H). Examination of day 18 ECMs cultures revealed that the cells were aligned and overlapping in an orderly manner and exhibited cord-like or trabecular type of cellular arrangement that resembled those of in vivo embryonic trabecular myocytes. The aligned myocytes showed the presence of developing sarcomeric units, which were positive for myosin and desmin (insets, Fig. 7A,B) and the transition of connexon proteins, C×45 to C×43 (Fig. 7G,H), indicative of progressive maturation and differentiation towards in vivo neonatal-like ventricular myocytes.

3.5.2. Characterization of GFP-labeled BMSCs in GFP-BMSCs/ECMs co-culture—In order to localize and characterize the phenotypic nature of differentiating BMSCs amidst and in the milieu of the developing ECMs, BMSCs were transfected with GFP-expressing lentivirus. Day 18 co-cultures harboring these GFP-BMSCs/ECMs were subjected to immunostaining and confocal microscopic analysis using the same battery of cardiomyogenic phenotypic markers as mentioned above. Similar to what was observed within ECMs only cultures, the GFP-marked BMSCs were positive for a variety of markers that are associated with differentiating cardiac myocytes such as cardiac α/β-MHC, sarcomeric MHC, cardiac cTnI, desmin, C×45, C×43 (Fig. 8A–L; Fig. 9A–L). Representative staining pattern and typical co-localization obtained for these cardiacrelated proteins within GFP-BMSCs/ECMs co-cultures are shown in Fig. 8A–L and Fig. 9(A–L).

In GFP-BMSCs/ECMs co-cultures the resident ECMs and untransformed GFP-BMSCs were distinguished from the transdifferentiated GFP-BMSCs by their lack of typical detectable colocalization signals. In this co-culture condition, the differentiating BMSCs appeared to be elongated and organized into interlacing bundles depicting varying degrees of cohesions and alignments (Fig. 8A–L). These multilayers of cells were composed of differentiating and maturing cardiac myocytes with evidence of nascent Z-dense bodies and the evolving cardiac specific structural organization that were positive for cardiac MHC and desmin (Fig. 8A–F) and the cardiac-related biosynthetic activities, BNP (Fig. 9A–C). In addition, these elongated GFP-BMSCs were in juxtaposition with ECMs and were mainly in parallel bundles but displayed the characteristic cross bridges to give a pseudosyncytial arrangement.

Nuclei of the cells were large, oval and/or round and centrally positioned (Fig. 8A–L; Fig. 9A–L). There were sites of specialized cell junctions in the form of connexon 45 and 43 gap junctions (Fig. 9G–L).

3.6. Ultrastructural morphology

The TEM analysis of ECMs showed typical ultrastructural morphological characteristics of developing embryonic cardiac myocytes for 15 days of development. Most of the cells revealed elongated centrally positioned nucleus and perinuclear cytoplasm consisting of numerous well-developed myofibrils with prominent sarcomeric units containing the Z-disks. A few of those myofibrils extended up to the marginal cytoplasm and formed the intercalated disk junctions with adjacent myocytes. In addition, these cells also contained numerous cytoplasmic mitochondria abutting the myofibrils (Fig. 10A). On the contrary, TEM analysis of quiescent BMSCs revealed ultrastructural morphology that appeared to be typical of a cell of mesenchymal origin. The predominantly population of cells exhibited centrally placed nuclei with highly dispersed out chromatin and nucleolus, indicative of an active cell. In addition, there were thin bundles of actin fibers (stress fibers) localized to the marginal cytoplasm. The central cytoplasm was characterized by numerous mitochondria and an extensive endoplasmic reticulum. The mitochondria appeared to be randomly dispersed with any discernable pattern of organization (Fig. 10B).

The differentiating cells in the ECMs/BMSCs co-culture expressed a unique cytoskeletal morphology, which was different from that seen in the negative control, BMSCs (BMSCs only culture) and the positive control, ECMs (ECMs only culture). These co-cultured cells expressed extensive bundles of thin fibers (actin fibers) being localized in both the marginal and central cytoplasm. These larger bundles of actin fibers now contained thick filaments and have numerous dense bodies (Fig. 10C,D), which were not seen in the BMSCs alone culture (Fig. 10B). However, thick filaments and dense bodies were seen in the ECMs' associated sarcomeres and myofibrils. These phenotypically altered cells also displayed many larger focal adhesions alone in the cell margins and more extensive junctional complexes resembling the structure of evolving rudimentary intercalated disk (Fig. 10C). In majority of cells, there were accumulations of dense bodies within the extensive bundles of thin and thick filaments. These dense bodies expressed a periodic spacing resembling the frequency of the spacing of Z lines (~2 μm) seen in the positive control ECM, indicative of nascent Z disks and sarcomeric formations (Fig. 10D). These dense bodies were prominently positive for desmin, the intermediate filament protein expressed by myogenic cells as shown by immunostaining and confocal microscopy, a corroborative finding (Fig. 8B,C). In addition, these complex bundles of filaments and associated dense bodies (Z-bodies) were also abutted by an extensive array of paralleloriented mitochondria similar to that seen abutting the myofibrils as in the case of positive control, ECMs.

4. Discussion

Here we report a reproducible in vitro 2-D model of mosaic cardiac tissue composed of two developmentally deferred distinct population of cells, ECMs (embryonic origin) and BMSCs (postnatal or adult origin) for exploring adult stem cell based myocardial regeneration that can be monitored for all aspects of cardiac regeneration, viz., electromechanical coupling

and neo-cardiomyocyte maturation, differentiation and integration. This mosaic of cardiac tissue generated in this co-culture conditions recapitulates many aspects of cell–cell (cardiac myocyte-stem cell) interactions that would be present in the heart during physiological and/or in pathological regenerations and address the controversial effects of adult BMSCs on myocardial regeneration during cellular cardiomyoplasty.

Previous reports provided substantial evidence that the adult BMSCs are capable of differentiating into both striated and nonstriated type of myocytes, including cardiac myocytes that may or may not have the intrinsic ability to undergo spontaneous beating and/or rhythmic contractions [15,26,33–36]. The in vitro directed differentiation of BMSCs towards cardiac myocyte lineage has been achieved under the influence of either the chemical and/or cellular cues [35–37]. In addition, it has been shown that BMSCs could differentiate into functioning cardiomyocyte-like cells when co-cultured in the milieu of various stages of developing cardiac myocytes, such as embryonic and neonatal cardiac myocytes, indicating that physical cell–cell interactions with cardiac myocytes is an essential component for the successful induction of BMSCs towards cardiomyogenic lineage [38–42]. However, these reports are not without controversy [43]. Recently, this notion is challenged by the fact that BMSCs have limited or no cardiomyogenic plasticity [44]. Collectively, these studies highlight the fact that BMSCs could be still the stem cell of choice for cellular cardiomyoplasty and, it warrants that a systematic approach encompassing many aspects of tissue regeneration and their mechanisms need to be addressed fundamentally. Hence, here we demonstrate that under appropriate in vitro combination of inductive cues (soluble and insoluble cellular interactions) BMSCs can be directed to differentiate into functioning cardiomyocyte-like cells. To achieve this aim, we developed a 2-D co-culture system in which a pure population of $CD90^+$ rat BMSCs was co-cultured with rat ECMs in myocyte medium on collagen-coated Petri dishes for differentiation and regeneration purposes. The putative $CD90^+$ BMSCs are multipotential and are capable of differentiating into cardiomyocyte-like, endothelial and smooth muscle cell lineages both in vitro as well as in vivo [15,26].

In general, successful in vitro differentiation depends on cell–cell as well as cell–matrix interactions [8,45]. Therefore, we examined the interaction of BMSCs with ECMs and their maturation and differentiation in myocyte medium alone (without any cardiogenic supplements) and, specifically investigated the nature and consequence of BMSCs physical contact with ECMs. And whether BMSCs were capable of exerting mechanical integration with EMCs and undergo spontaneous/or induced functional synchronization with ECMs and vice versa. As a control ECMs only cultures were assessed simultaneously. The ECMs only culture sustained the ECMs' in vitro continuum of differentiation and the cells progressively matured into neonatal type of myocytes, whereas, BMSCs/ECMs co-culture revealed that the cells have undergone synergistic and synchronized maturation and differentiation indicating that ECMs promoted the maturation and differentiation of BMSCs into cells characteristic of nascent cardiac myocytes.

One of the possible factors of contradictions in earlier studies of in vitro myogenic differentiation might be the result of the assumption that the contractile proteins are specific markers of overt myogenesis. Now, it is well established that a large variety of cells express

what was assumed typical muscle proteins, such as myosin or actin, and it appears that all contractile and regulatory proteins exist in isoprotein forms [46]. BMSCs itself constitutively express most of the myocyte related structural, contractile and junctional proteins at low to moderate levels [15]. Therefore to characterize the in vitro differentiation of rat ECMs and rat BMSC-derived neo-cardiomyocyte-like cells a battery of murine cardiomyogenic specific markers was employed in our study, and is mandatory when stem cells are employed and assessed for tissue-specific differentiation. The BMSCs/ECMs co-cultured cells were shown to express cardiac specific genes, proteins, ion channels and signal transduction machinery in a pattern that was comparable to the expression pattern of cultured ECMs cells and closely recapitulated the developmental pattern of in vivo neo-cardiomyogenesis. In addition, spontaneous and rhythmic contraction of these differentiating cells was evident in both BMSCs/ECMs co-culture and in ECMs only cultures over 14 days.

In any type of in vitro cellular differentiation, the cytodifferentiated cells need to be critically evaluated for their maturation and differentiation at transcriptional, translational and functional levels. Therefore, we examined the time-dependent expression pattern of various cardiac specific markers viz, Gata4, desmin, α-actinin, α/β-MHC, sMHC, cTnI, Cx45, Cx43, BNP of these cytodifferentiated cells. Since constitutive expression of these markers was detected at low to moderate levels in undifferentiated input BMSCs, it was used as calibrator control to quantitate the expression levels of cytodifferentiated cells. RT-qPCR results demonstrated that in vitro cardiomyogenic differentiation cultures of ECMs and BMSCs/ECMs for 18 days resulted in an augmented expression of mRNA transcripts coding for various cytoskeletal filament proteins that are associated with cardiac structural and contractile development such as α-actinin, α-MHC. β-MHC and troponin I. The maximal expression of all these contractile-associated mRNA appeared around day 6 followed by gradual downregulation and reached an apparent basal level around day 18 in both BMSCs/ECMs co-cultures as well as in control ECMs only cultures. The time-dependent downregulation of all these four structural/contractile filamental proteins in BMSCs/ECMs cocultures when compared with ECMs only cultures during this observed time period may be indicative of continual active cellular interaction, remodeling and development of the ECMs in correspondence with differentiating BMSCs. This emphasizes the fact that BMSCs were able to integrate mechanically with ECMs, which presumably the leading cause of cytoskeletal reorganization and transformation.

We further examined whether these augmented expression of mRNA transcripts coding for various cytoarchitectural proteins are in fact getting translated into structural and contractile proteins. As demonstrated by immunostaining for various cardiac specific markers, day 18 cultures revealed that ECMs as well as the cytodifferentiated BMSCs were able to undergo maturation and differentiation characteristics of a developing cardiac myocytes. In order to determine the exact fate of BMSCs amidst the developing ECMs, the BMSCs were labeled with either green or red fluorescent proteins and co-cultured for real-time observations of morphological transformation in correspondence with ECMs and for their subsequent analysis. Both ECMs and BMSCs/ECMs co-differentiating cells expressed cardiac α/β-MHC, cardiac cTnI, cardiac α-actinin and desmin. The cardiac specific transcription factor Gata4 was expressed by GFP-BMSCs and confirms the fact that around day 6 the BMSCs/ECMs co-cultured cells showed enhanced expression of Gata4 when compared with ECMs

only culture. In addition, these cells also expressed the junctional complex proteins, especially the gap junction proteins, C×45 and C×43 suggesting the existence of not only mechanical coupling but also electrical coupling among ECMs as well as between ECMs and BMSCs in co-culture condition. This is consistent with the observation that the differentiating BMSCs in the co-culture were able to beat and contract in synchrony with ECMs. The enhanced expression of these cardiac specific phenotypic proteins by majority of BMSCs, which were mechanically tethered to the ECMs suggest that BMSCs have the intrinsic myogenic potential to develop cardiac phenotype under appropriate inductive cues provided by the ECMs, and vice versa. All those isolated BMSCs that were probably not mechanically tethered to the existing ECMs expressed very low levels of cardiac specific proteins, and in fact demonstrated lack of rhythmic cellular contractions. Taken together, these observations suggest that physical cell-to-cell interactions in the form of intercellular communication are necessary to induce BMSCs towards cardiac phenotype.

Since terminally differentiated cardiac myocytes are highly specialized both structurally and functionally, we performed the contractility and calcium flux assays on these cultures by live cell confocal microscopy and imaging. Our results indicate that BMSCs were mechanically coupled with ECMs, and can undergo cyclic contractions essentially at the same frequency as those expressed by the ECMs. In addition, BMSCs' expressed a particular pattern and frequency of intracellular calcium oscillations, which was similar to the pattern and frequency of intracellular calcium oscillations observed in the case of ECMs', and is further suggestive of electrical coupling. These results indicate that the differentiating BMSCs are capable of developing the cellular machinery that is essential for their structural as well as contractile function. Moreover, this is the first ever documentation of calcium transients in the case of co-differentiating adult stem cell, BMSCs, mechanically coupled to ECMs.

Having established the cytodifferentiation of RFP-/GFP-BMSCs towards cardiac phenotype followed by the unambiguous demonstration of mechanical coupling, the pattern of contraction was validated further by morphometric analysis. In order to assess and delineate the cellular morphological changes of differentiating BMSCs, morphometric analysis was carried out on day 7 co-cultured cells. The obtained results indicate that BMSCs, which were mechanically associated with ECMs demonstrated nonrandom cyclic changes significantly dictated by the contraction frequency of the juxtaposed ECMs. On the contrary, all those isolated BMSCs that were probably not mechanically associated with the preexisting ECMs exhibited random non-cyclic changes naturally associated with routine cellular movements and migration. Hence, homotypic cellular adhesions and connexons may seem to be a prerequisite for cardiomyogenic induction and differentiation of these adult stem cells, BMSCs.

Finally, since cardiac myocytes have developmentally sophisticated cytoarchitectural elements, it is critically important to characterize the ultrastructural morphology of any stem cells that are directed to differentiate into cardiacmyocyte lineage. TEM analysis of the day 14 BMSCs/ECMs co-differentiating cells exhibited the typical appearance of differentiating cells developing the ultrastructural characteristics of early-state cardiac myocytes. These cells showed the earliest signs of overt myogenesis, the presumptive differentiating cells

became elongated, multilayered and displayed uniform registry. These aligned cells revealed bundles ofmyofibrils arranged in parallel orientation towards the long axis of the cells. There were numerous tightly packed strands of mitochondria running between the parallel bundles of myofibrils and some of it was located as subsarcolemmal clusters. In addition, the presence of rudimentary Z-dense bodies was seen amid the myofibrils indicative of nascent sarcomeric units of developing early-stage myocytes. The ultrastructural characteristics of these co-differentiating cells seem to give a momentary glimpse that ECMs are capable of undergoing partial dedifferentiation i.e. loss of contractile filaments as seen in the lower vertebrates such as fish and amphibians during regeneratory process [5]. The remodeling and reorganization of cytoarchitectural features of both BMSCs and ECMs in this co-culture condition suggest that both BMSCs and ECMs have the plasticity to reprogram in synchrony towards cardiomyogenic lineage and commitment and, essentially validates our previous findings observed in our 3-D co-culture system [15]. This phenomenon of partial dedifferentiation followed by redifferentiation of in vitro cardiac myocytes in the vicinity of adult bone marrow-derived stem cells may probably explain most of the discrepancies seen in the case of in vivo preclinical and clinical trials.

Further work is ongoing to investigate the influence of various chronotropic and ionotropic pharmacological agents on the contractile and electrophysiological response of this functioning mosaic of cardiac tissue. And examination of the global gene expression pattern of BMSCs and ECMs interaction to elucidate the subtle molecular mechanisms that are responsible for this unique type of cellular regeneration process seen in this co-culture condition.

5. Conclusions

Here we report a reproducible 2-D co-culture system that recapitulates many aspects of adult stem cell based myocardial regeneration. This 2-D model can be utilized to dissect various molecular mechanisms that are underpinning the adult BMSC based cellular cardiomyoplasty, especially, for the maintenance and repair of various cardiac lesions, such as ischemic heart disease (IHD), extrinsic/intrinsic cardiomyopathies, and cardiac atrophies. Moreover, this functioning mosaic of cardiac tissue can be of immense use for drug discovery and toxicity testing.

Acknowledgments

The authors thank Dr. Daping Fan for his enthusiastic and generous contributions of GFP/RFP lentiviruses and; Ms. Cheryl Cook and Ms. Lorain Junor for their excellent technical support, cell culture and myocyte isolation respectively. “This material is based upon work supported by the National Science Foundation/EPSCoR under Grant No. (EPS - 0903795).” - The South Carolina Project for Organ Biofabrication.

References

1. MacLellan WR, Schneider MD. Genetic dissection of cardiac growth control pathways. Annu Rev Physiol. 2000; 62:289–319. [PubMed: 10845093]
2. Rumyantsev PP. Evidence of regeneration of significant parts of myocardial fibers of frogs after trauma (Russian). Arkh Anat Gistol Embriol. 1961; 40:65–74. [PubMed: 13744704]

3. Rumyantsev PP. Post-injury DNA synthesis, mitosis and ultrastructural reorganization of adult frog cardiac myocytes. An electron microscopic-autoradiographic study. Z Zellforsch Mikrosk Anat. 1973; 139:431–50. [PubMed: 4541034]
4. Oberpriller JO, Oberpriller JC. Mitosis in the adult newt ventricle. J Cell Biol. 1971; 49:560–3. [PubMed: 19866784]
5. Oberpriller JO, Oberpriller JC. Response of the adult newt ventricle to injury. J Exp Zool. 1974; 187:249–60. [PubMed: 4813417]
6. Beltramin AP, Barlucchi L, Torella D, Baker M, Limana F, Chimenti S, et al. Adult cardiac stem cells are multipotent and support myocardial regeneration. Cell. 2003; 114:763–76. [PubMed: 14505575]
7. Messina E, De Angelis L, Frati G, Morrone S, Chimenti S, Fiordaliso F, et al. Isolation and expansion of adult cardiac stem cells from human and murine heart. Circ Res. 2004; 95:911–21. [PubMed: 15472116]
8. Carlson, BM. Principles of regenerative biology. Amsterdam: Elsevier; 2007. Stimulation of regeneration; p. 279-304.
9. Kehat I, Kenyagin-Karsenti D, Snir M, Segev H, Amit M, Gepstein A, et al. Human embryonic stem cells can differentiate into myocytes with structural and functional properties of cardiomyocytes. J Clin Invest. 2001; 108:407–14. [PubMed: 11489934]
10. Westfall MV, Pasyk KA, Yule DI, Samuelson LC, Metzger JM. Ultrastructure and cell-cell coupling of cardiac myocytes differentiating in embryonic stem cell cultures. Cell Motil Cytoskeleton. 1997; 36:43–54. [PubMed: 8986376]
11. Jackson KA, Majka SM, Wang H, Pocius J, Hartley CJ, Majesky MW, et al. Regeneration of ischemic cardiac muscle and vascular endothelium by adult stem cells. J Clin Invest. 2001; 107:1395–402. [PubMed: 11390421]
12. Orlic D, Kajstura J, Chimenti S, Jakoniuk I, Anderson SM, Li B, et al. Bone marrow cells regenerate infarcted myocardium. Nature. 2001; 410:701–5. [PubMed: 11287958]
13. Boyle AJ, Schulman SP, Hare JM. Is stem cell therapy ready for patients? Stem cell therapy for cardiac repair. Ready for the next step. Circulation. 2006; 114:339–52. [PubMed: 16864739]
14. Makino S, Fukuda K, Miyoshi S, Konishi F, Kodama H, Pan J, et al. Cardiomyocytes can be generated from marrow stromal cells in vitro. J Clin Invest. 1999; 103:697–705. [PubMed: 10074487]
15. Valarmathi MT, Goodwin RL, Fuseler JW, Davis JM, Yost MJ, Potts JD. A 3-D cardiac muscle construct for exploring adult marrow stem cell based myocardial regeneration. Biomaterials. 2010; 31:3185–200. [PubMed: 20129663]
16. Liechty KW, MacKenzie TC, Shaaban AF, Radu A, Moseley AM, Deans R, et al. Human mesenchymal stem cells engraft and demonstrate site-specific differentiation after in utero transplantation in sheep. Nat Med. 2000; 6:1282–6. [PubMed: 11062543]
17. Shake JG, Gruber PJ, Baumgartner WA, Senechal G, Meyers J, Redmond JM. Mesenchymal stem cell implantation in a swine myocardial infarct model: engraftment and functional effects. Ann Thorac Surg. 2002; 73:1919–25. [PubMed: 12078791]
18. Toma C, Pittenger MF, Cahill KS, Cahill KS, Byrne BJ, Kessler PD. Human mesenchymal stem cells differentiate to a cardiomyocyte phenotype in the adult murine heart. Circulation. 2002; 105:93–8. [PubMed: 11772882]
19. Chen SL, Fang WW, Ye F, Liu YH, Qian J, Shan SJ, et al. Effect on left ventricular function of intracoronary transplantation of autologous bone marrow mesenchymal stem cell in patients with acute myocardial infarction. Am H Cardiol. 2004; 94:92–5.
20. Min JY, Sullivan MF, Yang Y, Zhang JP, Converso KL, Morgan JP, et al. Significant improvement of heart function by cotransplantation of human mesenchymal stem cells and fetal cardiomyocytes in postinfarcted pigs. Ann Thorac Surg. 2002; 74:1568–75. [PubMed: 12440610]
21. Aggarwal S, Pittenger MF. Human mesenchymal stem cells modulate allogeneic immune cell responses. Blood. 2005; 105:1815–22. [PubMed: 15494428]
22. Janssens S, Dubois C, Bogaert J, Theunissen K, Deroose C, Desmet W, et al. Autologous bone marrow-derived stem-cell transfer in patients with ST-segment elevation myocardial infarction: double-blind, randomized controlled trial. Lancet. 2006; 14:113–21. [PubMed: 16413875]

23. Cleland JG, Freemantle N, Coletta AP, Clark AL. Clinical trials update from the American heart association: REPAIR-AMI, ASTAMI, JELIS, MEGA, REVIVE-II, SURVIVE, and PROACTIVE. Eur J Heart Fail. 2006; 8:105–10. [PubMed: 16387630]
24. Zimmet JM, Hare JM. Emerging role for bone marrow derived mesenchymal stem cells in myocardial regenerative therapy. Basic Res Cardiol. 2005; 100:471–81. [PubMed: 16237508]
25. Valarmathi MT, Yost MJ, Goodwin RL, Potts JD. A three-dimensional tubular scaffold that modulates the osteogenic and vasculogenic differentiation of rat bone marrow stromal cells. Tissue Eng. 2008; 14:491–504.
26. Valarmathi MT, Davis JM, Yost MJ, Goodwin RL, Potts JD. A three-dimensional model of vasculogenesis. Biomaterials. 2009; 30:1098–112. [PubMed: 19027154]
27. Simpson DG, Terracio L, Terracio M, Price RL. Modulation of cardiac myocyte phenotype in vitro by the composition and orientation of the extracellular matrix. J Cell Physiol. 1994; 161:89–105. [PubMed: 7929612]
28. Rosen, S.; Skaletsky, HJ. Primer3 on the WWW for general users and for biologist programmers. In: Krawetz, S.; Mlsener, S., editors. Bioinformatics methods and protocols: methods in molecular biology. Totowa, NJ: Human Press; 2000. p. 365-86.
29. Pfaffl MW. A new mathematical model for relative quantification in real-time RT-PCR. Nucleic Acids Res. 2001; 29:e45. [PubMed: 11328886]
30. Valarmathi MT, Yost MJ, Goodwin RL, Potts JD. The influence of proepicardial cells on the osteogenic potential of marrow stromal cells in a three-dimensional tubular scaffold. Biomaterials. 2008; 29:2203–16. [PubMed: 18289664]
31. Reyes M, Dudek A, Jahagirdar B, Koodie L, Marker PH, Verfaillie CM. Origin of endothelial progenitors in human postnatal bone marrow. J Clin Invest. 2002; 109:337–46. [PubMed: 11827993]
32. Dominici M, Le Blanc K, Mueller I, Slaper-Cortenback I, Marini F, Krause D, et al. Minimal criteria for defining multipotent mesenchymal stromal cells. The International Society For Cellular Therapy position statement. Cytotherapy. 2006; 8:315–7. [PubMed: 16923606]
33. Wakitani S, Saito T, Caplan AI. Myogenic cells derived from rat bone marrow mesenchymal stem cells exposed to 5-azacytidine. Muscle Nerve. 1995; 18:1417–26. [PubMed: 7477065]
34. Pittenger MF, Mackay AM, Beck SC, Jaiswal RK, Douglas R, Mosca JD, et al. Multilineage potential of adult human mesenchymal stem cells. Science. 1999; 284:143–7. [PubMed: 10102814]
35. Wang JS, Shum-Tim D, Galipeau J, Chedrawy E, Eliopoulos N, Chiu RC. Marrow stromal cells for cellular cardiomyoplasty: feasibility and potential clinical advantages. J Thorac Cardiovasc Surg. 2000; 120:999–1005. [PubMed: 11044327]
36. Fukuda K. Development of regenerative cardiomyocytes from mesenchymal stem cells for cardiovascular tissue engineering. Artif Organs. 2001; 25:187–93. [PubMed: 11284885]
37. Martin-Rendon E, Sweeney D, Lu F, Girdlestone J, Navarrete C, Watt SM. 5- Azacytidine-treated human mesenchymal stem/progenitor cells derived from umbilical cord, cord blood and bone marrow do not generate cardiomyocytes in vitro at high frequencies. Vox Sang. 2008; 95:137–48. [PubMed: 18557828]
38. Koninckx R, Hensen K, Daniels A, Moreels M, Lambrichts I, Jongen H, et al. Human bone marrow stem cells co-cultured with neonatal rat cardiomyocytes display limited cardiomyogenic plasticity. Cytotherapy. 2009; 11:778–92. [PubMed: 19878064]
39. Gallo MP, Ramella R, Alloatti G, Penna C, Pagliaro P, Marcantoni A, et al. Limited plasticity of mesenchymal stem cells cocultured with adult cardiomyocytes. J Cell Biochem. 2007; 100:86–99. [PubMed: 16888800]
40. Wang T, Xu Z, Jiang W, Ma A. Cell-to-cell contact induces mesenchymal stem cell to differentiate into cardiomyocyte and smooth muscle cell. Int J Cardiol. 2006; 109:74–81. [PubMed: 16122823]
41. Xu M, Wani M, Dai YS, Wang J, Yan M, Ayub A, et al. Differentiation of bone marrow stromal cells into the cardiac phenotype requires intercellular communication with myocytes. Circulation. 2004; 110:2658–65. [PubMed: 15492307]

42. He XQ, Chen MS, Li SH, Liu SM, Zhong Y, McDonald Kinkaid HY, et al. Coculture with cardiomyocytes enhanced the myogenic conversion of mesenchymal stromal cells in a dose-dependent manner. Mol Cell Biochem. 2010; 339:89–98. [PubMed: 20063193]

43. Rose RA, Jiang H, Wang X, Helke S, Tsoporis JN, Gong N, et al. Bone marrow-derived mesenchymal stromal cells express cardiac-specific markers, retain the stromal phenotype, and do not become functional cardiomyocytes in vitro. Stem Cells. 2008; 26:2884–92. [PubMed: 18687994]

44. Rose RA, Keating A, Backx PH. Do mesenchymal stromal cells transdifferentiate into functional cardiomyocytes? Circ Res. 2008; 103:e120. [PubMed: 18948624]

45. Even-Ram S, Yamada KM. Cell migration in 3D matrix. Curr Opin Cell Biol. 2005; 17:524–32. [PubMed: 16112853]

46. Perry, SV. Variation in the contractile and regulatory proteins of the myofibril with muscle type. In: Milhorat, AT., editor. Exploratory concepts in Muscular Dystrophy. Vol. II. Amsterdam: Excerpta Medica; 1994. p. 319-28.

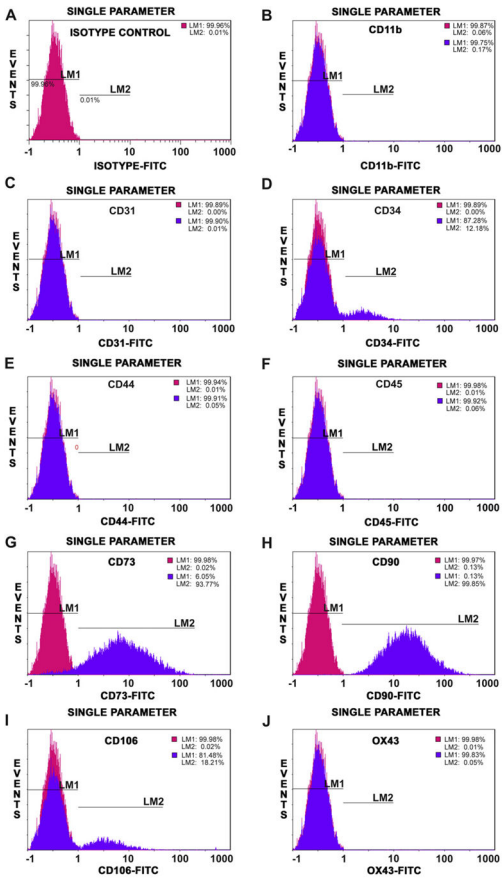

Fig. 1.

Immunophenotyping of undifferentiated rat BMSCs by flow cytometry. Single parameter histograms showing the relative fluorescence intensity of staining (abscissa) and the number of cells analyzed, events (ordinate). Isotype controls were included in each experiment to identify the level of background fluorescence (Panel A). The intensity and distribution of cells stained for hematopoietic and endothelial markers; CD11b, CD31, CD34, CD44, CD45, CD106 and OX43 (purple, shaded peaks) were not significantly different from those of isotype control (pink, shaded peaks) (Panels B–F, I,J), indicating that these cultures were devoid of any potential hematopoietic and/or endothelial cells of bone marrow origin. The fluorescent intensity was greater (shifted to right) when BMSCs were stained with CD73 and CD90 (purple) compared to isotype control (pink) (Panels G, H). The predominant population of BMSCs consistently expressed CD73 and CD90 surface molecules, a property of rat bone marrow-derived mesenchymal/stromal stem cells.

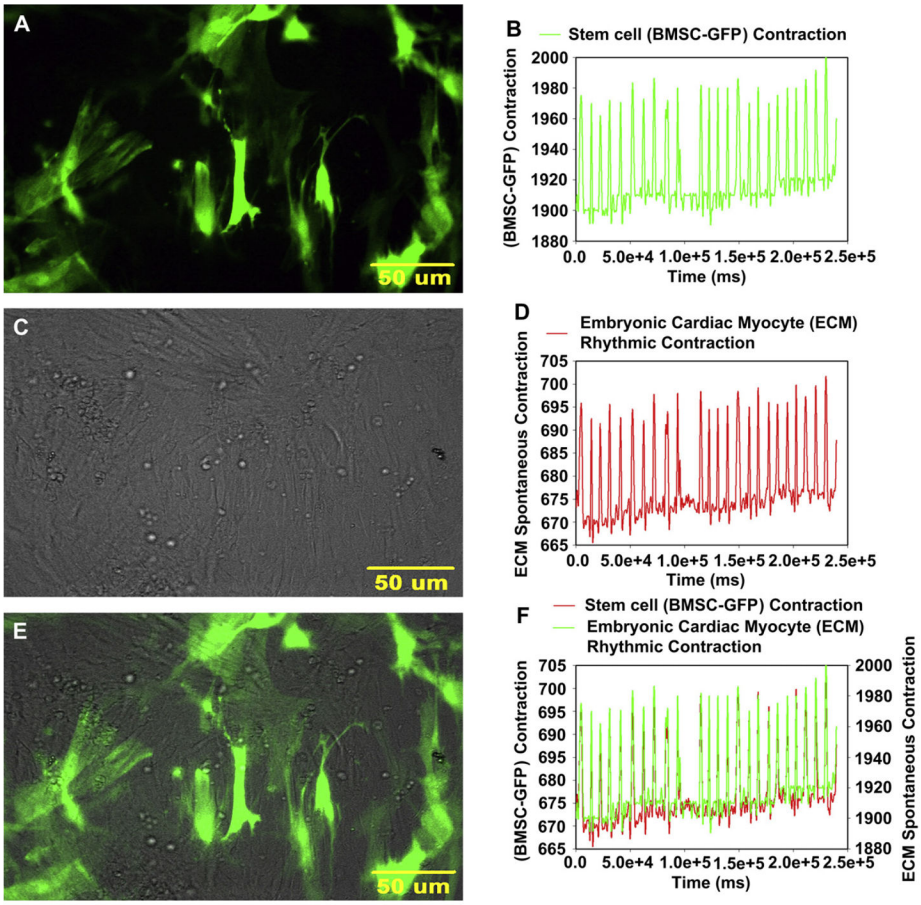

Fig. 2.

Contractility assay of ECMs/GFP-BMSCs co-cultured in myocyte medium. GFP-BMSCs were tethered to ECMs and were mechanically coupled at the same frequency of ECMs contractions. The frequency of cellular movement of BMSC was technically determined by ECM contractile frequency. (A) Representative fluorescence image of green fluorescent protein labeled BMSCs (GFP-BMSCs) attached to ECMs. BMSCs were elongated and assumed prolate spheroid morphology. (B) The pattern and frequency of BMSC cellular movement and contraction. (C) Representative phase contrast image of GFP-BMSCs tethered to ECMs. (D) The pattern and frequency of ECM rhythmic contraction. (E) Overlay of fluorescent and phase contract images depicting relative positions of GFP-BMSCs and ECMs in this co-culture. (F) Comparison of the pattern of GFP-BMSC cellular movement with the pattern of ECM contractility revealed that the frequency of movement of BMSC was essentially the same and determined by the frequency of ECM contractions.

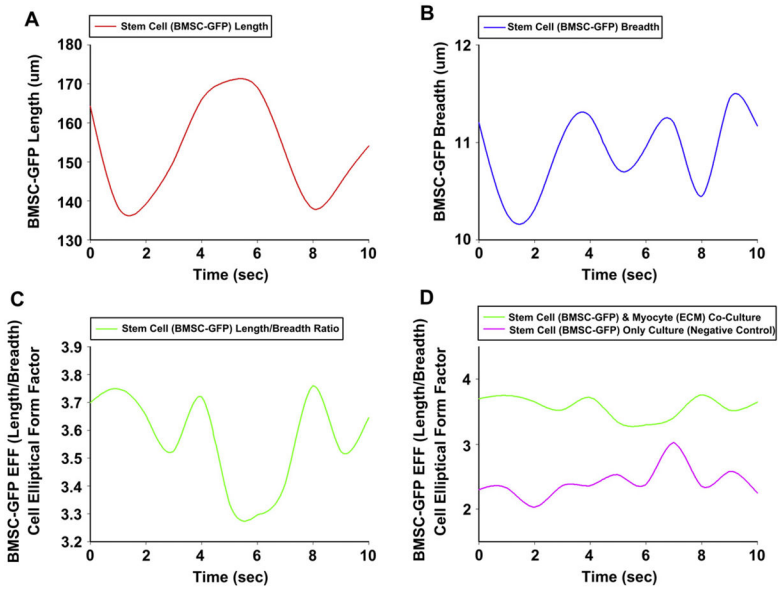

Fig. 3.

Morphometric analysis of ECMs/GFP-BMSCs cultured in myocyte medium. The descriptors of changes in cell shape and morphological transformation viz., cellular morphological parameters: length - L {L}, breadth - B {B}, and the elliptical form factor – EFF {L/B} were measured by the imaging software for each thresholded and image isolated cell. Values of L, B, and EFF were calculated directly from the integrated morphometry subroutine of MetaMorph 6.1 image analysis software. Representative example of the changes in morphological parameters viz., L, B, and EFF of a GFP-BMSC that was mechanically attached to a spontaneously contracting ECM. (A) Change in {L} of a GFP-BMSC that was attached to a ECM. (B) Change in {B} of the same GFP-BMSC in panel A. Changes in {B} were variable and was not appear to be directly associated with changes in {L}. (C) The EFF {ratio of L/B} was periodic with variable amplitude and indicated that the GFP-BMSC was under physical deformation of elongation and relaxation. (D) Comparison of EFF of a GFPBMSC that was in co-culture and mechanically attached to a spontaneously contracting ECM (green line) with a quiescent GFP-BMSC alone that was not in physical contact with a spontaneously contracting ECM (pink line). The quiescent GFP-BMSC exhibited only modest non-periodic changes in EFF that were associated with natural cell migration and movement. The GFP-BMSC that was in physical contact with an ECM exhibited a greater EFF indicative of a change in morphology, which undergoes cyclic changes of contraction and relaxation.

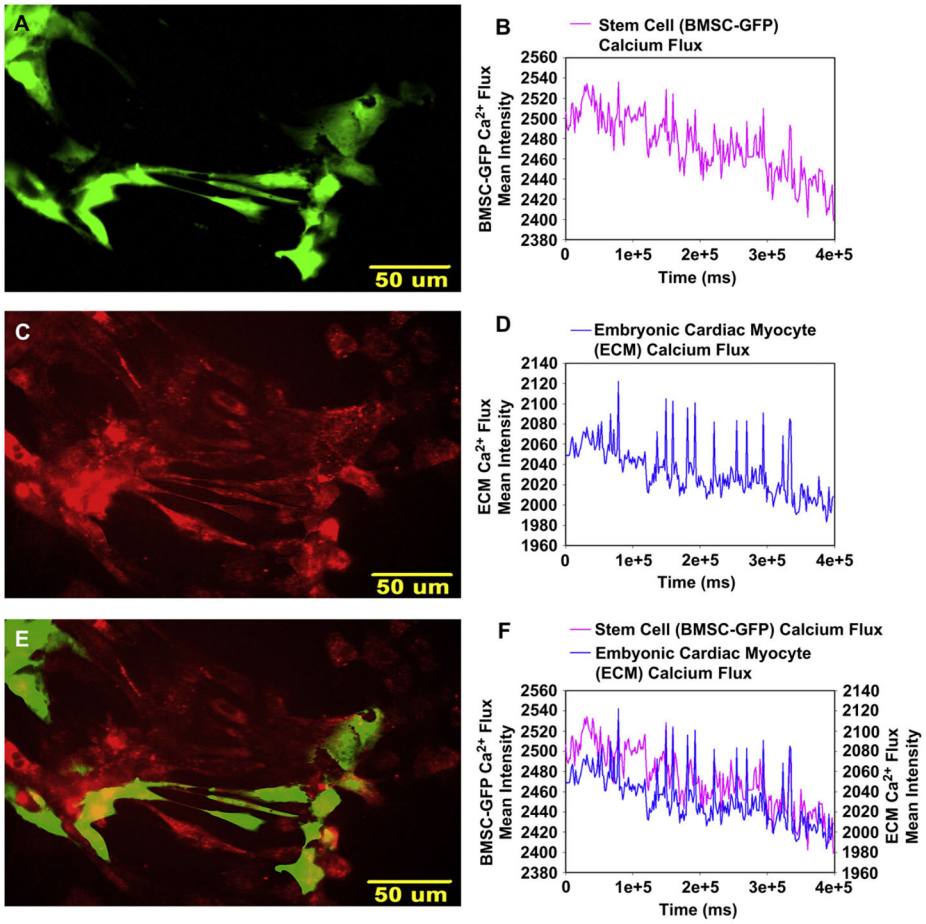

Fig. 4.

Calcium flux assay of ECMs/GFP-BMSCs co-cultured in myocyte medium. GFP-BMSCs were mechanically coupled with spontaneously contracting ECMs revealed intracellular calcium flux with similar frequency but smaller amplitude. (A) Green fluorescent protein tagged BMSCs (GFP-BMSCs) were labeled with the calcium indicator, Calcium Orange and imaged in the green channel. (B) The pattern of GFP-BMSC intracellular calcium oscillations measured in the red channel for Calcium Orange. (C) ECMs and GFP-BMSCs were labeled with Calcium Orange and imaged in the red channel. (D) The pattern of contracting ECM intracellular calcium oscillations measured in the red channel for Calcium Orange. (E) Overlay of green channel image of GFP-BMSCs labeled with the calcium indicator, Calcium Orange and red channel image of ECMs and GFP-BMSCs labeled with Calcium Orange in this co-culture. (F) Comparison of the pattern of GFP-BMSC calcium flux with the pattern of contractile ECM displayed that the intracellular oscillation of calcium of BMSC was essentially the same as that of ECM but with relatively smaller spikes.

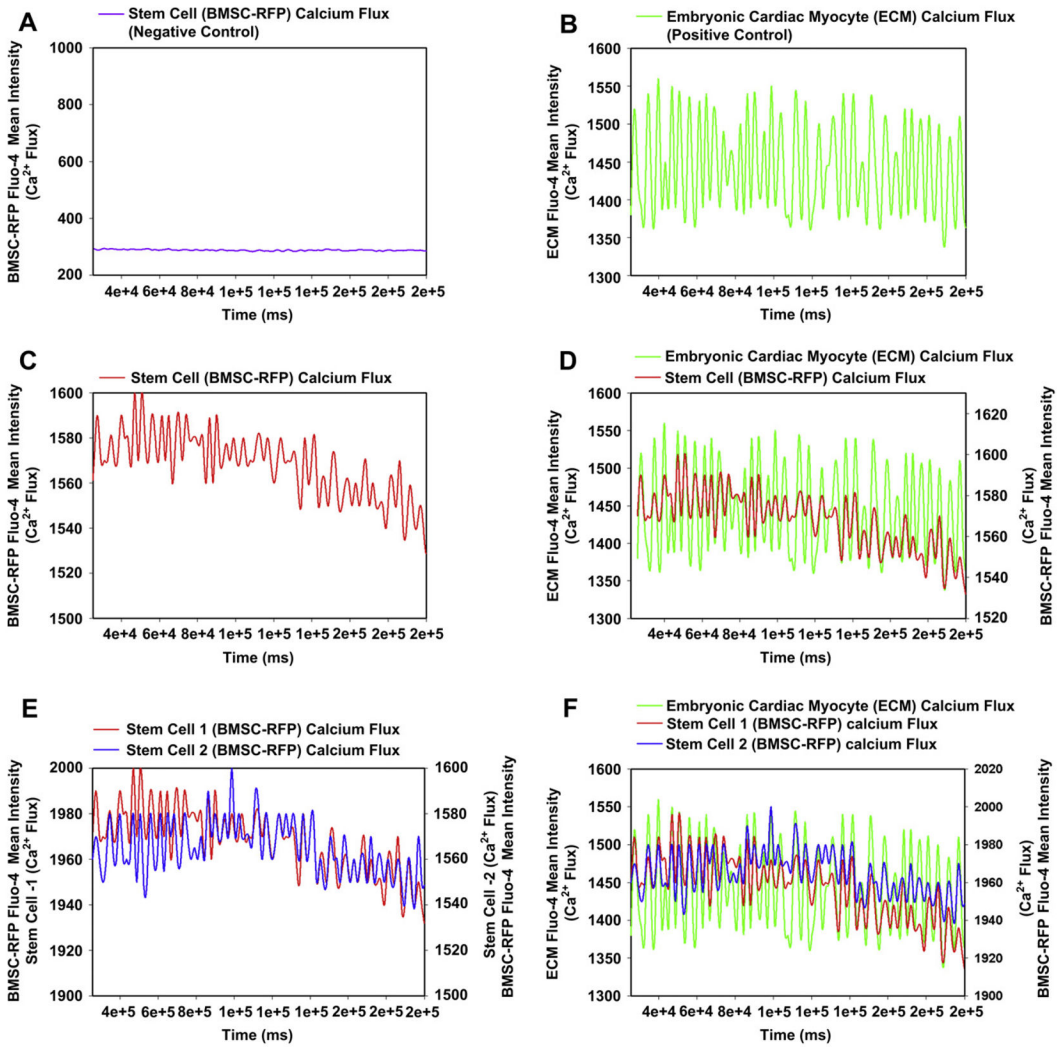

Fig. 5.

Calcium flux assay of ECMs/RFP-BMSCs co-cultured in myocyte medium. Comparison of calcium flux in quiescent RFP-BMSC not physically in contact with an ECM (negative control), in spontaneously contracting ECMs (positive control), and multiple RFP-BMSCs mechanically connected to a single ECM. Red fluorescent protein tagged BMSCs (RFPBMSCs) and ECMs were labeled with the calcium indicator, Fluo-4 and imaged in the green channel. (A) The pattern of intracellular calcium oscillations of quiescent RFP-BMSC that was not mechanically associated with ECM revealed a non-periodic frequency with very small amplitude peaks. (B) The typical pattern of intracellular calcium oscillations of a spontaneously contracting ECM. (C) The pattern of intracellular calcium oscillations of RFP-BMSC that was mechanically coupled with an ECM became periodic with a significant increase in amplitude. (D) Comparison of the pattern of calcium flux of an RFP-BMSC that was mechanically associated with a spontaneously contracting ECM. The frequency of RFPBMSC intracellular calcium oscillations was essentially the same as that of the ECM, but relatively at a lower amplitude. (E) Comparison of the patterns of calcium flux of two individual RFP-BMSCs that were mechanically associated with the same ECM but not in

contact with each other. The frequency of intracellular calcium oscillations in these two RFP-BMSCs exhibited essentially the same periodicity with minor variations, and amplitudes of the same order of magnitude. (F) The two RFP-BMSCs that were in contact with the same ECM demonstrated the same periodic frequency of intracellular calcium flux as seen associated with the myofibrillar contractions in the ECM. This suggests that ECM and its two interacting RFP-BMSCs were electromechanically coupled to each other.

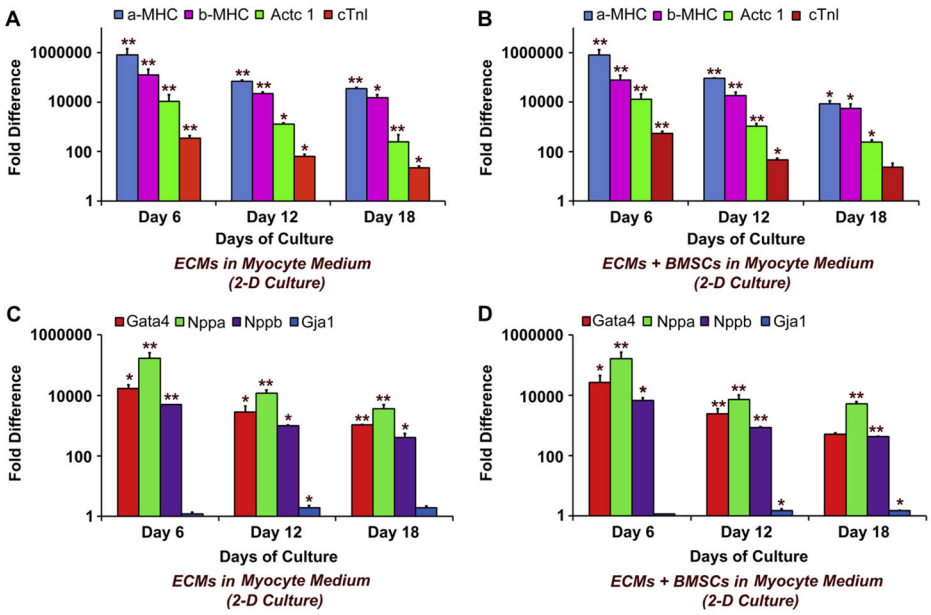

Fig. 6.

Real-time reverse transcriptase quantitative polymerase chain reaction (RT-qPCR) analysis of various key cardiogenic markers, α-MHC (myosin, heavy chain6, cardiac muscle, alpha - Myh6), β-MHC (myosin, heavy chain 7, cardiac muscle, beta - Myh7), α-actin cardiac (actin, alpha, cardiac muscle 1 - Actc1), cTnI (troponin I type 3, cardiac - Tnni3), Gata4 (GATA binding protein 4 - Gata4), Nppa (natriuretic peptide precursor A – ANP), Nppb (natriuretic peptide precursor B – BNP) and Gja1 (gap junction protein, alpha 1 – C×43) as a function of time (abscissa). ECMs cultured in collagen-coated culture dishes (2-D culture) in myocyte medium (A, C). ECMs and BMSCs co-cultured in collagen-coated culture dishes (2-D culture) in myocyte medium (B, D). The calibrator control included BMSCs day 0 sample and; the target gene expression was normalized by a non-regulated reference gene expression, Arbp. The expression ratio (ordinate) was calculated using the REST-XL version 2 software. The values are mean ± standard error of the mean for three independent cultures ($n = 3$), *$p < 0.05$; **$p < 0.001$.

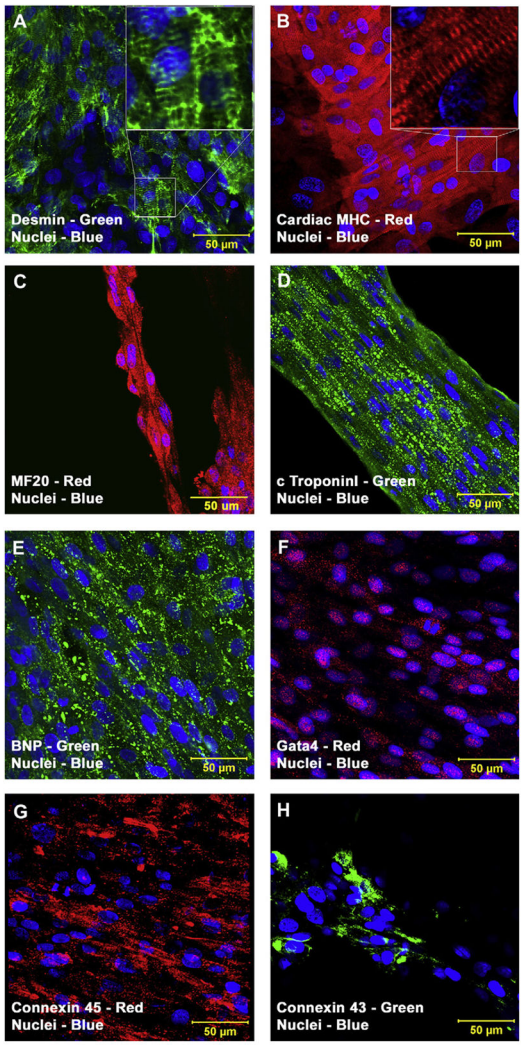

Fig. 7.

Expression pattern of various cardiomyogenic markers in ECMs containing cultures by confocal microscopy. Localization of key cardiac myocyte phenotypic markers of day 18 embryonic cardiac myocyte (ECM) cultures in myocyte medium demonstrated the expression of cardiac specific structural and contractile proteins, desmin (A), α/β-MHC (B), sMHC (C), cTnI (D), peptide hormone, BNP (E), transcription factor, Gata4 (F), and the gap junction proteins, C×45 and C×43 (G, H). Immunostaining of ECMs cultures in myocyte medium showed foci of elongated and/or round to polyhedral type of cells arranged in multilayered clusters and organized into cord-like or trabecular type of cellular arrangement (A–H). Majority of these ECMs were aligned and overlapping in an orderly manner (B–H). Inset in panel A, exhibits that desmin is predominantly localized in the Z lines of the myocyte, revealing a marked striped appearance. Inset in panel B, reveals early-forming myofibrillar sarcomeric units and the characteristic cross-striations. Nuclei of these cells were large and either oval or round in appearance and were centrally positioned. Cells were also stained for nuclei (blue, DAPI). Image (G) shows a projection representing 10 sections collected at 1 µm intervals (9 µm). Merged images (A–H). (A–H, scale bar 50 µm).

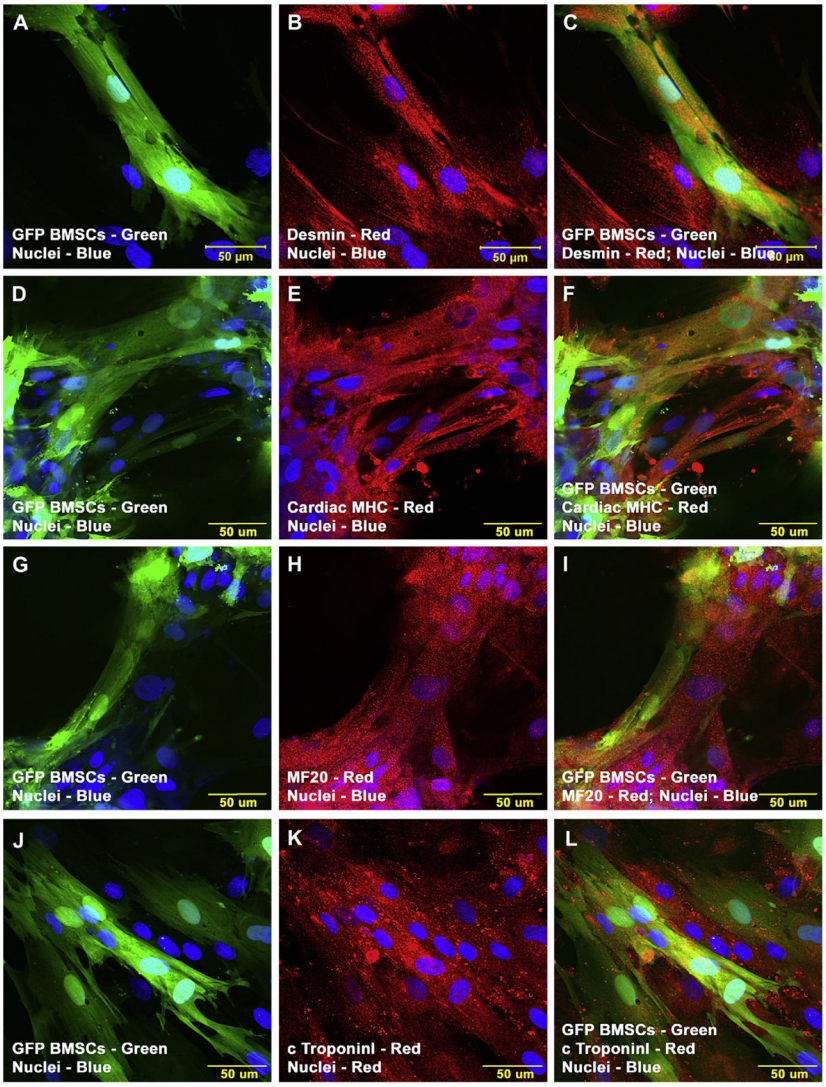

Fig. 8.

Expression pattern of various cardiogenic markers in GFP-BMSCs/ECMs containing cultures by confocal microscopy. Localization of key cardiac myocyte phenotypic markers of day 18 embryonic cardiac myocytes (ECMs) and green fluorescent protein labeled bone marrow stromal cells (GFP-BMSCs) co-cultures in myocyte medium demonstrated the expression of structural and contractile proteins, desmin (B, C), α/β-MHC (E, F), sMHC (H, I), and cTnI (K, L). The transdifferentiated GFP-BMSCs were delineated by their colocalization signals (orange to yellow). The trabeculae of cells were arranged in a pseudosyncytial pattern (A–L). Nuclei of these cells were large and either oval or round in appearance and were centrally located. Cells were also stained for nuclei (blue, DAPI) and GFP-BMSCs (green, GFP). Merged images (A–L). (A–L scale bar 50 µm).

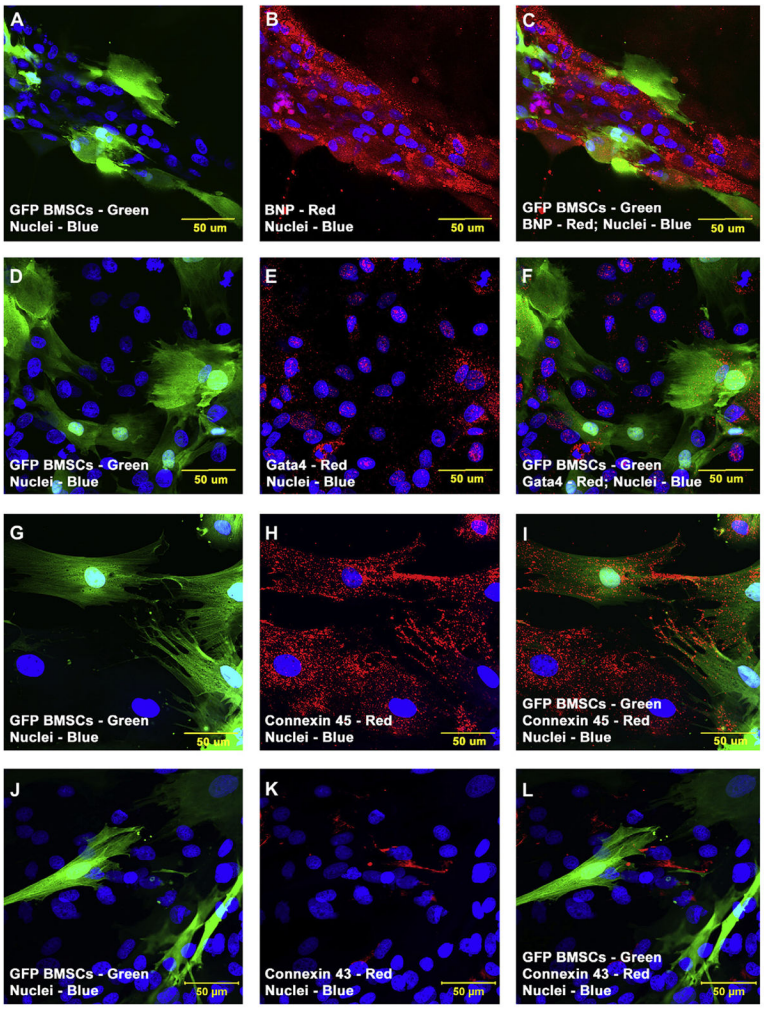

Fig. 9.

Expression pattern of various cardiogenic markers in GFP-BMSCs/ECMs containing cultures by confocal microscopy. Localization of key cardiacmyocyte phenotypic markers of day18 embryonic cardiacmyocytes (ECMs) and green fluorescent protein labeled bone marrow stromal cells (GFP-BMSCs) co-cultures in myocyte medium demonstrated the expression of peptide hormone, BNP (B,C), transcription factor, Gata4 (E,F), and the gap junction proteins, C×45 (H,I) and C×43 (K,L). The transdifferentiated GFP-BMSCs were delineated by their colocalization signals (orange to yellow). Most of these co-differentiating cells appeared as foci of single and/or multilayered cell clusters and displayed the characteristic pseudosyncytial arrangement (A–C). These co-differentiating cells displayed specialized cell junctions (H–I, K–L). Nuclei of these cells were large and either oval or round in appearance and were centrally located. Cells were also stained for nuclei (blue, DAPI) and GFP-BMSCs (green, GFP). Merged images (A–L). (A–L scale bar 50 μm).

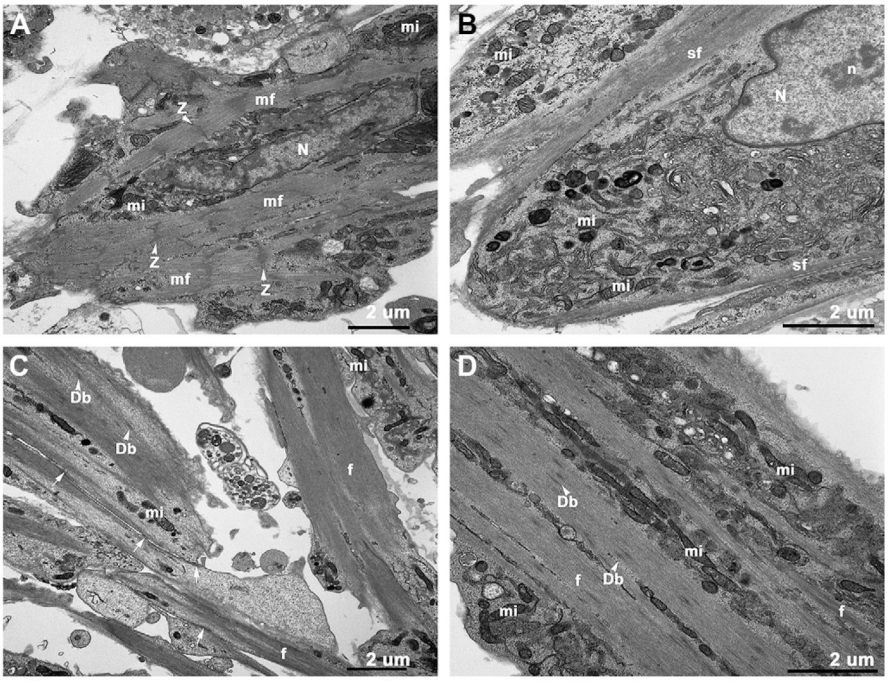

Fig. 10.

Transmission electron microscopic (TEM) analysis of day 14 BMSCs, ECMs, and ECMs/BMSCs cultures. (A) ECM cultured in myocyte medium showed elongated nucleus (N). The cytoplasm revealed myofilaments and myofibrils (mf), perinuclear early sarcomeric units, Z-disks (Z) and numerous mitochondria (mi). (B) BMSC cultured under the same culture conditions revealed large nucleus (N) with nucleolus (n) and the central cytoplasm was characterized by numerous mitochondria and extensive endoplasmic reticulum, the ultrastructural characteristics of active, immature cells. In addition, the BMSC cytoskeleton was characterized by bundles of actin stress fibers (sf) predominantly localized towards the peripheral cytoplasm. These bundles of actin fibers appeared to be very uniform and devoid of any detectable dense bodies. Numerous focal adhesions were localized along the margins of adjacent BMSCs. (C) BMSCs/ECMs co-cultured under similar culture conditions demonstrated a unique cytoskeletal morphology that was obviously different from that observed in the controls viz., BMSCs (Panel B) and ECMs (Panel A). There were bundles of actin stress fibers localized in both the peripheral and central cytoplasm. These extensive bundles of actin fibers now contained thick filaments and numerous dense bodies (Db, arrow heads). The thick and think filaments showed association with these dense bodies or plaques. In addition these cells had many larger focal adhesions (arrows) and more extensively developed junctional complexes resembling the structure of rudimentary intercalated disk. (D) In addition, majority of cells in BMSCs/ECMs co-culture conditions developed larger and extensive fiber bundles. Within these extensive bundles of fibers displayed accumulation of dense bodies which expressed a periodic spacing resemble the frequency of the spacing of Z lines (~2 μm) as seen in the positive control, ECM (Panel A). These complex bundles of filaments were abutted by extensive parallel-oriented mitochondria similar to that seen bordering the myofibrils of the positive control, ECM (Panel A).

Table 1

Primary antibodies used in this study.

Primary antibodies	Dilutions	Source	Cell target
BMSCs characterization markers			
CD11b	1:50	BD Pharmingen	Leukocytes
CD31	1:10	Abcam	Endothelial
CD34	1:50	Santa Cruz Biotechnology	Endothelial
CD44	1:10	Gene Tex, Inc	Leukocytes
CD45	1:50	BD Pharmingen	Hematopoietic
CD73	1:50	BD Pharmingen	BMSCs
CD90	1:50	BD Pharmingen	BMSCs
CD106	1:50	BD Pharmingen	Endothelial
OX43	1:10	Gene Tex, Inc	Endothelial
Cardiac myocyte differentiation markers			
Sarcomere myosin (MF20)	1:200	DSHB	Cardiomyocyte
Cardiac myosin heavy chain (a/b-MHC)	1:200	Abcam	Cardiomyocyte
Cardiac troponin I (cTnI)	1:200	Santa Cruz Biotechnology	Cardiomyocyte
Connexin 45 (Cx45)	1:200	Santa Cruz Biotechnology	Cardiomyocyte
Connexin 43 (Cx43)	1:200	Santa Cruz Biotechnology	Cardiomyocyte
Desmin	1:200	Abcam	Cardiomyocyte
GATA4	1:200	Santa Cruz Biotechnology	Cardiomyocyte
BNP	1:200	Santa Cruz Biotechnology	Cardiomyocyte

Table 2

RT-qPCR primer sequences used in this study.

Genes	Forward primer	Reverse primer	Product length (bp)	Annealing temperature (°C)	GenBank accession No
Myh6	5′–TGATGACTCCGAGGAGCTTT–3′	5′–TGACACAGACCCTTGAGCAG–3′	234	58	NM_017239.2
Myh7	5′-CCTCGCAATATCAAGGGAAA-3′	5′-TACAGGTGCATCAGCTCCAG-3′	198	58	NM_017240.1
Actc1	5′–CACGGCATTATCACCAACTG–3′	5′–AACAATGCCTGTGGTTCTCC–3′	240	58	NM_019183.1
Tnni3	5′-ACGTGGAAGCAAAAGTCACC-3′	5′-CCTCCTTCTTCACCTGCTTG-3′	201	58	NM_017144.1
Gata4	5′-TCAAACCAGAAAACGGAAGC-3′	5′-CTGCTGTGCCCATAGTGAGA-3′	192	58	NM_144730.1
Nppa	5′-ATACAGTGCGGTGTCCAACA-3′	5′-CGAGAGCACCTCCATCTCTC-3′	209	58	NM_012612.2
Nppb	5′-GGAAATGGCTCAGAGACAGC-3′	5′-CGATCCGGTCTATCTTCTGC-3′	164	58	NM_031545.1
Gja1	5′-TCCTTGGTGTCTCTCGCTTT-3′	5′-GAGCAGCCATTGAAGTAGGC-3′	167	58	NM_012567.2
Arbp	5′–CGACCTGGAAGTCCAACTAC–3′	5′–ATCTGCTGCATCTGCTTG–3′	109	58	NM_022402.1